AGU PUBLICATIONS

JGR

Journal of Geophysical Research: Space Physics

RESEARCH ARTICLE
10.1002/2013JA019466

Key Points:
- Scintillations in relation to equatorial electrodynamics
- Variability of EEJ and scintillation
- Equatorial irregularity

Correspondence to:
S. K. Chakraborty,
skchak2003@yahoo.com

Citation:
Chatterjee, S., S. K. Chakraborty, B. Veenadhari, and S. Banola (2014), A study on ionospheric scintillation near the EIA crest in relation to equatorial electrodynamics, *J. Geophys. Res. Space Physics*, *119*, 1250–1261, doi:10.1002/2013JA019466.

Received 20 SEP 2013
Accepted 16 JAN 2014
Accepted article online 20 JAN 2014
Published online 12 FEB 2014

A study on ionospheric scintillation near the EIA crest in relation to equatorial electrodynamics

S. Chatterjee[1], S. K. Chakraborty[1], B. Veenadhari[2], and S. Banola[2]

[1]Department of Physics, Raja Peary Mohan College, Uttarpara, India, [2]Indian Institute of Geomagnetism, Navi Mumbai, India

Abstract Equatorial electrojet (EEJ) data, which are considered as a proxy index of equatorial electric field, are analyzed in conjunction with equatorial ionosonde, total electron content (TEC) and scintillation data near the equatorial ionization anomaly (EIA) crest for the equinoctial months of high solar activity years (2011–2012) to identify any precursor index of postsunset evolution of equatorial electron density irregularities and subsequent occurrence of scintillation near the northern EIA crest. Only geomagnetically quiet and normal electrojet days are considered. The diurnal profiles of EEJ on the scintillation days exhibit a secondary enhancement in the afternoon to presunset hours following diurnal peaks. A series of electrodynamical processes conducive for generation of irregularities emerge following secondary enhancement of EEJ. Latitudinal profile of TEC exhibits resurgence in EIA structure around the postsunset period. Diurnal TEC profile near the EIA crest resembles postsunset secondary enhancement on the days with afternoon enhancement in EEJ. Occurrence of equatorial spread *F* and postsunset scintillation near the EIA crest seems to follow the secondary enhancement events in EEJ. Both the magnitude and duration of enhanced EEJ are found to be important for postsunset intensification of EIA structure and subsequent occurrence of equatorial irregularities. A critical value combining the two may be considered an important precursor for postsunset occurrence of scintillation near the EIA crest. The results are validated using archived data for the years 1989–1990 and explained in terms of modulation effects of enhanced equatorial fountain.

1. Introduction

Occurrence of ionospheric scintillations is one of the main hindrances for faithful maintenance of transionospheric communication and navigation links, particularly around the crest of the equatorial ionization anomaly (EIA). Most severe scintillations occur in the postsunset period of the equinoctial months of high solar activity years. Scintillations are produced by irregularities in electron density distribution. Though much study has been made on the climatology of scintillation the day-to-day variability in generation of ionospheric irregularity giving rise to equatorial scintillation has remained an unresolved issue over many decades [*Basu et al.*, 2002, 2009]. The present study is an attempt to identify a precursor signature for triggering the irregularity processes leading to scintillation near the EIA crest in the context of variability of equatorial electrodynamics as revealed through diurnal variation of equatorial electrojet (EEJ)

The EEJ is referred to a belt of enhanced *E* region current around the magnetic equator. During daytime the zonal electric field developed in the *E* region near the magnetic equator owing to neutral winds plays the pivotal role in modulating the dynamical behavior of the equatorial ionosphere. The Pedersen current due to the eastward electric field and the eastward current due to the vertical Hall voltage combine to cause an equatorial electrojet (EEJ) [*Cowling*, 1933]. It is manifested by deflections in the magnetometer reading representing variations of the horizontal intensity of the Earth's magnetic field measured in the equatorial region. The *E* layer plasma which is confined to quasi horizontal geomagnetic field lines [*Abdu et al.*, 2003] is the origin of EEJ. The field lines connect the equatorial *F* region at higher altitudes to conjugate *E* layers that enables strong electrical coupling between the two regions. The *E* region fields thus transmitted to the *F* region produce the $\mathbf{E}\times\mathbf{B}$ drift that lifts the *F* region plasma at higher altitudes. The uplifted plasma simultaneously diffuses down the magnetic field lines to form the crests of the equatorial ionization anomaly (EIA) around ±15° magnetic latitudes. The upward $\mathbf{E}\times\mathbf{B}$ drift and downward diffusion of plasma acting together at all points along the field lines produce the EIA mainly by removing the plasma from around the equator. Only a small part of the downward diffusing plasma accumulates around the EIA crests due to lack of support and most of it diffuses further down and gets lost by chemical recombination at lower altitudes [*Balan et al.*, 2013]. The daytime electric field, primarily controlled by *E* region dynamo [*Heelis*, 2004], is the driving force for both the vertical plasma drift

and the EEJ, in addition the EEJ strength is influenced by the *E* region conductivity [*Kelley*, 1989]. However, the day-to-day variations of the conductivity are less prominent than those of the *E* field [*Stolle et al*., 2008]. The EEJ is taken as proxy index of equatorial electric field [*Anderson et al*., 2002].

The importance of the electric field as revealed through EEJ in modulating the electrodynamical behavior of the equatorial ionosphere is reported through numerous studies [*Sethia et al*., 1980; *Rastogi and Klobuchar*, 1990; *Anderson et al*., 2002]. The EIA is directly controlled by the field related to EEJ strength [*MacDougall*, 1969; *Stolle et al*., 2008]. *Deshpande et al*. [1977] showed a strong EIA on a day with strong EEJ and the absence of EIA on a day when no EEJ developed. *Rastogi and Klobuchar* [1990] found an approximately linear dependence between crest to trough total electron content (TEC) ratio and the EEJ strength.

In the early evening hours, a unique feature of the equatorial and low-latitude ionosphere is the prereversal enhancement (PRE) in the vertical ion velocity that occurs shortly after local sunset, superimposed on the typical diurnal variation of daytime upward and nightside downward drift [*Fesen et al*., 2000]. Importance of daytime EEJ in modulating the postsunset behavior of the equatorial ionosphere through the development PRE of eastward electric field is reported through several studies [*Sastri*, 1998; *Dabas et al*., 2003; *Kelley et al*., 2009]. The EEJ and the *F* region neutral wind dynamo combine in setting up a current system which determines the low-latitude equatorial electric fields during the evening hours [*Haerendel and Eccles*, 1992]. Normal PRE is suggested to be created by partial EEJ current closure which is reported to be the dominant mechanism for the onset of PRE [*Kelley et al*., 2009]. *Sastri* [1998] has shown that the abnormally large postsunset height rise of the equatorial *F* layer followed by intense equatorial spread *F* is due to the enhanced noontime EEJ strength, even during low solar activity period.

The PRE of the eastward electric field is of crucial importance for destabilization of the ionosphere to generate irregularities of various scale sizes giving rise to equatorial spread *F* (ESF) and hence scintillations of satellite signals [*Farley et al*., 1970; *Woodman*, 1970; *Basu et al*., 1996; *Fejer et al*., 1999]. The electric field related to PRE leads to a resurgence of the EIA in the postsunset period thereby developing ambient conditions conducive for occurrence of scintillations at frequencies as high as 4 GHz around the EIA crests during solar maximum [*Basu et al*., 1987, 2002]. In the EIA region the occurrence of equatorial scintillation at higher latitudes is conditional on their prior appearance at lower latitudes. The low-latitude belt is primarily controlled by the generation, growth, and dynamics of scintillation producing irregularities over the magnetic equator [*Basu et al*., 1978; *Somayajulu et al*., 1984; *Dabas and Reddy*, 1986]. The bubbles and associated irregularities, after its onset over the magnetic equator, reach the highest altitudes/latitudes only on those days when postsunset secondary maximum in TEC, which is a measure of ambient ionization, is observed there [*Basu et al*., 1987; *Chakraborty et al*., 1999; *Dabas et al*., 2003] in addition to high values of *F* layer virtual height ($h'F$) and bubble rise velocity. A linear relationship between the crest to trough ratio of the EIA NmF2 and PRE [*Whalen*, 2000, 2003] with the afternoon (1400–1700 LT) drift having the effect of steepening the slope of the linear trend at various solar activity levels is reported by *McDonald et al*. [2011]. *Park et al*. [2010] reported that the plasma vertical drift component corresponding to PRE is determined by (i) the presunset dynamo current strength and (ii) local time gradient of *E* region conductivity. The current system responsible for the occurrence of PRE is an extension of the daytime one which gets extended into the postsunset equatorial region to meet the demand of current continuity of the postsunset *F* region dynamo [*Prakash et al*., 2009]. An elevated EEJ in the afternoon sector and its persistence may be advantageous to meet the current continuity requirement, thereby, facilitating the PRE evolution.

Several workers reported importance of the presunset ionospheric conditions to dictate the postsunset occurrence of ESF/scintillations [*Raghavarao et al*., 1988; *Sridharan et al*., 1994; *Basu et al*., 2002; *Uemoto et al*., 2010]. On the days of normal EEJ *Hajra et al*. [2012] reported that EEJ variations around the noontime period may not consistently dictate the day-to-day variability of postsunset equatorial irregularity. On the contrary afternoon variation of eastward electric field as revealed through EEJ was qualitatively suggested to be the important parameter leading to postsunset resurgence of EIA and subsequent evolution of spread *F* irregularities in the low-latitude zone. Only a few days data pertaining to vernal equinoctial months were used for the study. In the present investigation occurrence of ESF/scintillation is studied in a quantitative way, using a larger data base corresponding to solar cycle 24, in the context of variation EEJ as well as ambient ionization level as revealed through TEC. An attempt is made to suggest threshold values of some parameters which may fruitfully be used as forecasting indices for the occurrence of equatorial electron density irregularities and subsequent

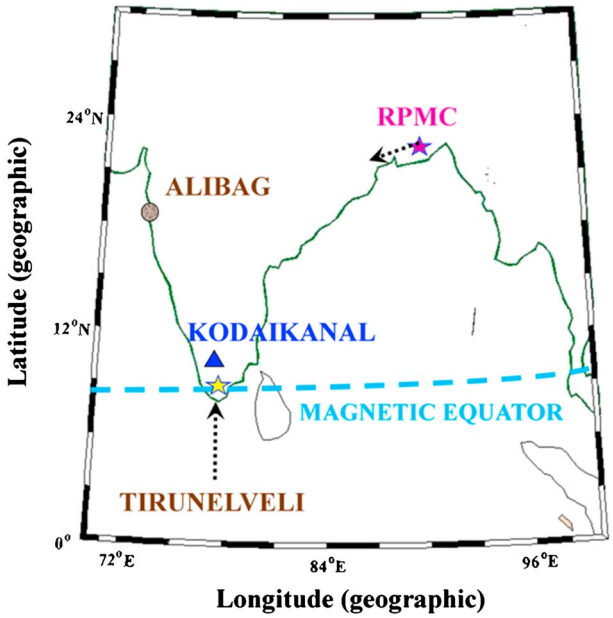

Figure 1. Geographic locations of the VHF observing station: RPMC (22.66°N, 88.4°E) along with the ionosonde centre at two equatorial stations Tirunelveli (geographic: 8.73°N, 77.7°E) and Kodaikanal (geographic: 10.2°N, 77.5°E), and nonequatorial magnetometer station Alibag (geographic: 18.64°N, 72.87°E). Arrow indicates VHF subionospheric (at 350 km altitude) location of RPMC (21.1°N, 86.9°E).

onset of scintillation near the EIA crest. The results are also validated using database of high solar activity period of 1989–1990, pertaining to different solar cycle 22.

2. Data

Ionospheric scintillations at VHF frequency (250 MHz) recorded at Raja Peary Mohan College centre (RPMC: geographic: 22.66°N, 88.36°E; geomagnetic: 13.12°N, 161.69°E; dip: 33.5°), situated near the northern crest of EIA, are studied for the present investigation. The 350 km pierce point of satellite Fleet Satellite Communications (FSC) exhibiting VHF scintillations is located at (21.1°N, 86.9°E). Global Navigation Satellite Systems (GNSS) scintillations and Total Electron Content (TEC) data are also recorded from RPMC using a dual frequency Septentrio PolaRxS-Pro receiver. An elevation mask angle of 50°, appropriate for slant to vertical conversion, is selected for TEC estimation at 1 min interval. For scintillation recording an elevation mask angle of 20° is selected to avoid multipath effects. S_4 index, normalized standard deviation of signal intensity, is estimated using the standard method [*Whitney et al*., 1969] and is being used to express scintillation strength.

The strength of EIA structure and corresponding variability are studied using International GNSS Service (IGS) TEC data obtained from the Coordinated Data Analysis Web data.

Magnetometer horizontal intensity (*H*) data recorded at Tirunelveli (8.73°N, 77.7°E, dip: 0. 5°) and Alibag (18.64°N, 72.87°E; dip 23°) are used to estimate EEJ following the method suggested by *MacDougall* [1969] and *Chandra and Rastogi* [1974]. Tirunelveli is an electrojet station, while Alibag is located outside the EEJ belt. The data at 1 min interval are used for estimating EEJ. Ionosonde h′F data of Tirunelveli are used to estimate plasma drift velocity and signature of ESF near the magnetic equator. It is assumed that during postsunset hours when the *F* layer is above a threshold height of about 300 km the vertical plasma drift velocity calculated from ionosonde data obtained from an equatorial station may correspond to real $\mathbf{E}\times\mathbf{B}$ drift velocity [*Bittencourt and Abdu*, 1981]. It should be mentioned that scintillation observing station (RPMC), magnetometer and ionosonde locations are not along the same meridian (Figure 1). There is a longitude difference of (~10°), large enough for point-to-point correspondence but the general features may be assumed to be the same [*Chakraborty et al*., 1999; *Ray et al*., 2006; *Chakraborty and Hajra*, 2009; *Hajra et al*., 2009].

The period of observation pertains to equinoctial months of high solar activity years (2011–2012) when occurrence probability of scintillation is much larger. $F_{10.7}$ solar flux varies in the range 121–190 solar flux unit (10^{-22} W m^{-2} Hz^{-1}) pertaining to solar cycle 24. Only the geomagnetically quiet days with $Dst > -50$ nT [*Akasofu*, 1981] and normal electrojet days are considered.

3. Results

Equatorial electrojet (EEJ) data in conjunction with TEC and scintillation data around the northern crest of equatorial ionization anomaly (EIA) for the period of 25 March to 25 April 2011, 20 September to 12 November 2011, and 20 March to 16 April 2012 are analyzed in the present investigation. Total number of days in the observation period of equinoctial months is 110. The dates are limited due to unavailability of EEJ data. The period of investigation includes 80 magnetically quiet days out of which normal electrojet (NEJ) days are 57. The EEJ is considered as a proxy index of equatorial *E* region electric field which is the main

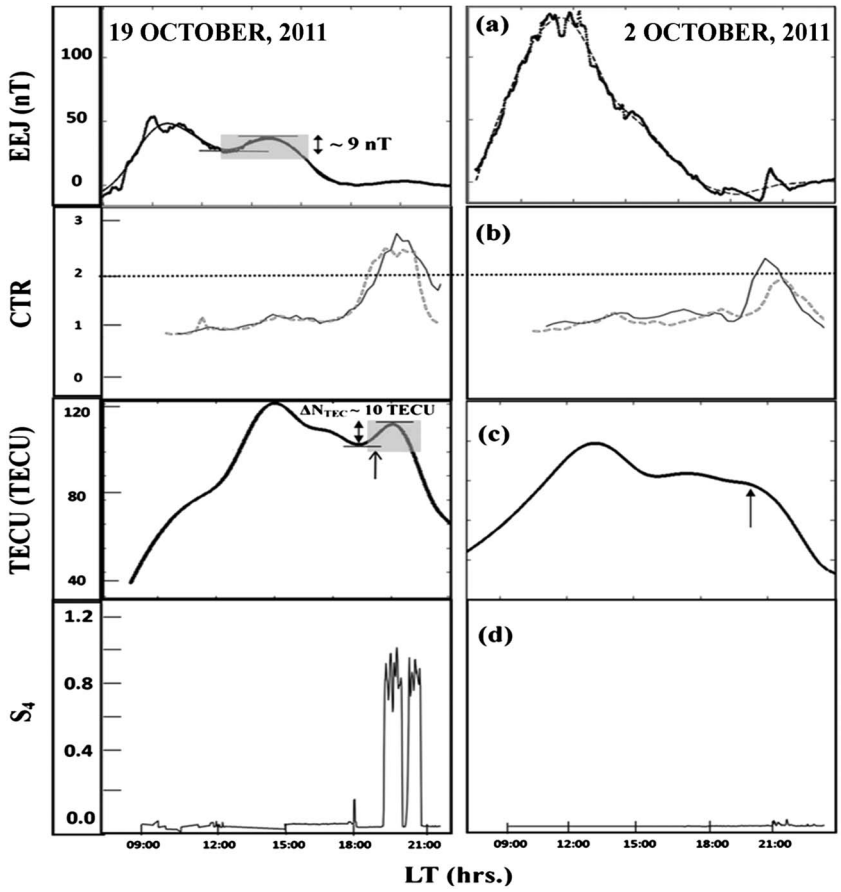

Figure 2. Diurnal variations of (a) EEJ, (b) CTR at 75°E (dotted line), and 85°E (solid plot) longitudes, (c) TEC at RPMC and (d) scintillation strength S_4 at VHF obtained at RPMC on 19 October 2011 (left) and 2 October 2011 (right). Solid (dashed) plot in Figure 2a represents original (smooth fit) data. Shaded portion in Figures 2a and 2c pertains to appearance of secondary enhancement in EEJ and TEC, respectively (shown by double headed arrow). Vertical arrow in Figure 2c indicates VHF subionospheric sunset time (LT h). Dotted horizontal line in Figure 2b corresponds to CTR value ~ 2.0.

ingredient of equatorial fountain. The results of investigation on EEJ in the context of generation/inhibition of electron density irregularities responsible for scintillation near the EIA crest during the period of NEJ are presented in the following sections.

One of the important features detected in the diurnal profile of EEJ is the evolution of an afternoon (14:30–8:00 IST h) enhancement following the diurnal maximum. It is observed for ~ 89% cases of total NEJ days. The magnitude of the enhancement is estimated following the dip in the smooth fit of the afternoon distribution up to the secondary peak of the same as shown in Figure 2a. The duration of the afternoon enhancement is calculated from full width at half maximum. The estimated magnitude and duration of the secondary enhancement are found to be in the range ~ 2–14 nT and ~ 15–190 min, respectively. It may be mentioned that variability in EEJ around the afternoon hours for the non-ESF days lies in the range ~ ± 0.51 to ±1.30 nT. Figure 2a is a sample plot showing signature of enhancement (magnitude ~ 9 nT) in the diurnal EEJ profile during afternoon hours following the diurnal peak on 19 October 2011, whereas no such distinctive feature in the temporal evolution pattern of EEJ is detected on 2 October 2011 (Figure 2a). The emergence of secondary enhancement of EEJ seems to have dominant modulating effects on the equatorial ionosphere that is reflected in the several ionospheric parameters. A secondary enhancement in EEJ signifies intensification of equatorial fountain in the late afternoon hours facilitating development of enhanced EIA structure. Temporal evolution pattern of crest to trough ratio (CTR), representing the strength of ionization anomaly are plotted for the two days in Figure 2b. It is estimated using IGS TEC data at 75°E and 85°E longitudes pertaining approximately to the locations of

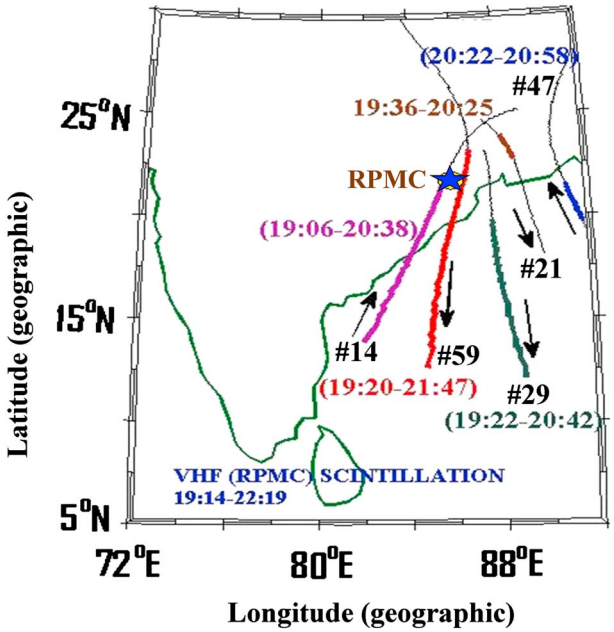

Figure 3. Tracks of GNSS satellites (geographic) around the observing station and corresponding VHF subionospheric location of RPMC are shown for 19 October 2011. Pseudorandom noise (PRN) codes of the satellites and scintillation timing of the corresponding L1 band scintillation are provided for each track. Bold portions of the respective tracks represent scintillation occurrence.

magnetometer and VHF subionospheric point (Figure 1), respectively. A clear signature of strongly developed postsunset ionization anomaly is reflected on 19 October 2011, while emergence of a weaker EIA is evident on 2 October 2011. The diurnal profile of TEC at RPMC, located near the EIA crest, exhibits postsunset secondary enhancement on 19 October 2011, while no such increase is conspicuous on 2 October 2011 (Figure 2c). The enhanced amplitude is observed to lie in the range between 3 and 20 TECU (total electron content unit, 1 TECU = 10^{16} el m^{-2}) in most of the cases. The enhancement magnitude is estimated following the same method as used for the EEJ. Afternoon strengthening of equatorial fountain, as revealed through enhanced EEJ field and subsequent intensification of EIA structure leading to persistence of elevated ambient ionization level near the EIA crests set up favorable conditions for development of electron density irregularity as revealed through occurrence of ESF and postsunset scintillations near the EIA crest. In the ionosonde data strong-range type postsunset spread *F* is observed on 19 October 2011. Postsunset VHF scintillations are recorded at RPMC on 19 October 2011, while no such signatures are observed on 2 October 2011 (Figure 2d). Figure 3 is a plot of different satellite tracks exhibiting scintillation at L1 frequency of the GPS, GLONASS, and Satellite Based Augmentation System (SBAS) links on the days of VHF scintillation (19 October 2011), while no such scintillation event is conspicuous on the other day. Communication/Navigation Outage Forecasting System (C/NOFS) satellite in situ measurements are used to forecast ambient plasma densities and irregularities in the equatorial ionosphere [*de La Beaujardière et al*. 2004]. C/NOFS has a low-inclination (13°) orbit, with perigee of 400 km and apogee of 850 km. Figure 4 reveals signature of distinct plasma density depletion around the Indian longitude sector along with the trace of multiple bubble structures within the depletion region in the postsunset period during C/NOFS orbit number 19041 on 19 October 2011. No such characteristic feature indicating trace of plasma density depletion during C/NOFS orbit number 18789 is detected on 2 October 2011. All these features demonstrate a coherent picture of the Indian equatorial ionosphere that seems to emerge following afternoon intensification in EEJ.

Following the case study, a statistical study is made to investigate the correspondence among various sequential ionospheric events following afternoon secondary enhancement in EEJ. During the observation period the latitudinal distribution of TEC obtained from IGS data sets corresponding to 85°E longitude zones has been analyzed. The evening anomaly peak appears in most of the cases around the region ~ 20°–22.5°N latitude following secondary enhancement in post afternoon EEJ, while on the other days, the anomaly peak is recorded to be developed around ~ 12.5°–17.5°N. A new parameter, ΔH_{EEJ}, obtained by multiplying the product of enhancement magnitude and time duration of EEJ enhancement is introduced. The importance of not only the elevated field strength but also its persistence is revealed through the parameter. The afternoon EEJ enhancement parameter (ΔH_{EEJ}), not merely the peak amplitude, bears a good correspondence (correlation ~ 0.62 at 1% significance level) with the postsunset crest TEC amplitude. The afternoon-enhanced EEJ field appears to be a precursor signature of the resurgence of evening anomaly leading to an elevated level of ionization density around the crest region.

An intensified EIA structure results in secondary enhancement in the diurnal profile of TEC near the EIA crest around postsunset period. An effort is made to study the possible correspondence between the secondary

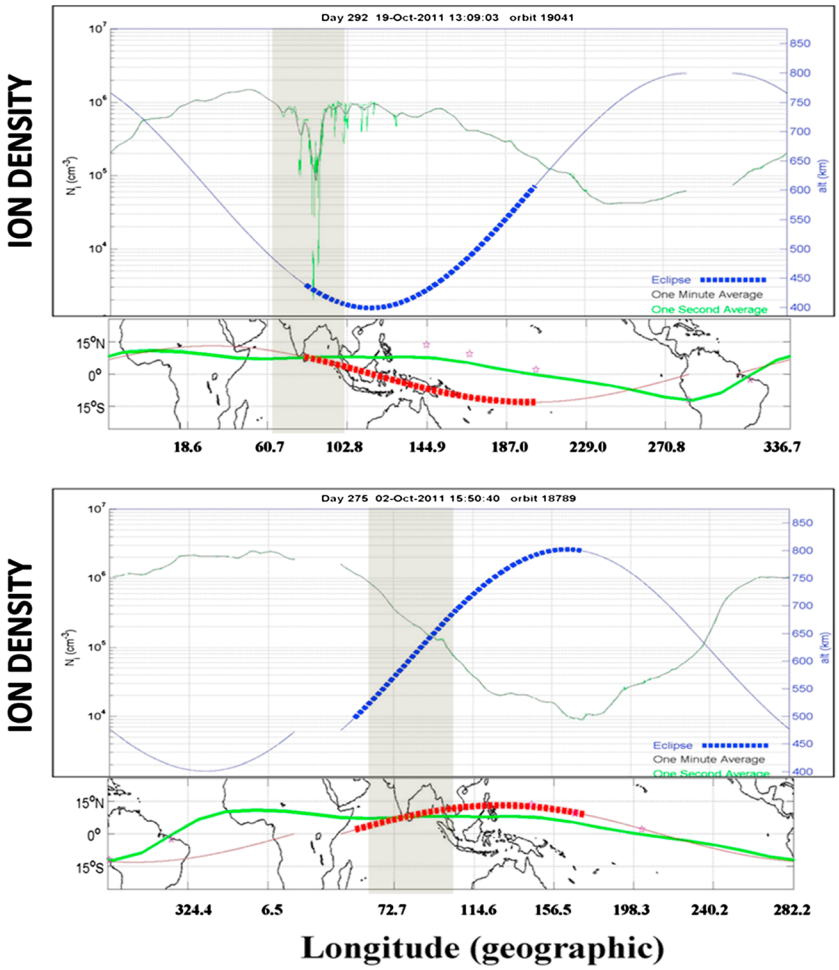

Figure 4. Track and ion density variation as detected by C/NOFS satellites (orbit number embedded in corresponding figures) with longitude and altitude. Shaded region indicates the presence and absence of plasma depletion structure/bubble on (a) 19 October 2011 (~ 1930 IST h) and (b) 2 October 2011 (~ 2130 IST h), respectively, over the Indian longitude zone.

enhancement in the afternoon EEJ and the corresponding enhancement in TEC. A statistical analysis indicates a significant positive correlation ~ 0.63 between the magnitudes of the secondary enhancement of EEJ and postsunset increase in Vertical Total Electron Content (VTEC) (ΔN_{TEC}) (Figure 5a). A more statistically significant correlation ~ 0.89 is reflected when ΔH_{EEJ} parameters (nT-min) are investigated in conjunction with ΔN_{TEC} (Figure 5b). Thus, the magnitudes as well as the duration of secondary enhancement of EEJ, as reflected through ΔH_{EEJ} parameter may be considered an important index to modulate the postsunset equatorial electrodynamic leading to enhanced ΔN_{TEC}.

The onset of equatorial spread *F* (ESF) is observed over the magnetic equator at Tirunelveli (geographic latitude: 8.73°N, longitude: 77.7°E, dip: 0.5°) following secondary enhancement in EEJ for ~ 94% cases. Ionosonde data at the equatorial station (Tirunelveli) for the ESF days are analyzed to study the equatorial *F* region ionospheric conditions following secondary enhancement in the afternoon EEJ field. A rise in *F* layer height, h′F, is evident for all cases during 1830–1950 IST (h) preceding the onset of ESF. Vertical plasma drift velocity is calculated from d (h′F)/dt in successive 10 min interval. Ionosonde data recorded maximum h′F values during the postsunset period to lie in the range ~ 300–506 km. The estimated plasma drift velocity may thus be assumed to represent real $\mathbf{E} \times \mathbf{B}$ drift velocity [*Bittencourt and Abdu*, 1981] and is calculated to be in the range ~ 20–83 m/s. Non-ESF days correspond to absence/suppressed secondary enhancement of afternoon EEJ with a reduced value of ΔH_{EEJ} parameter < 300 (nT-min) in some cases. For these cases postsunset h′F predominantly lie in the range ~ 227–354 km and the plasma drift velocity is estimated to be <15 m/s for all cases.

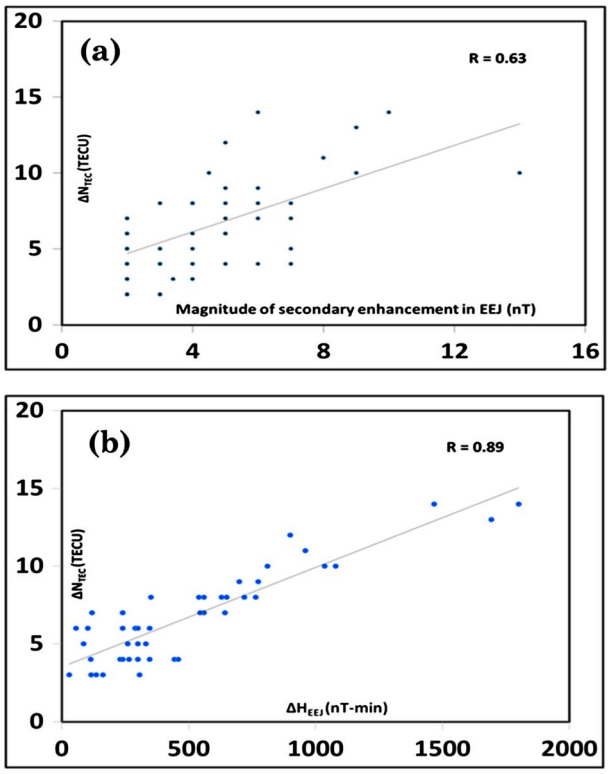

Figure 5. Plots of (a) secondary enhancement amplitude of EEJ and TEC (ΔN_{TEC}) near the EIA crest and (b) ΔH_{EEJ}, obtained by multiplying magnitude and duration of enhancement versus ΔN_{TEC}.

A combined study involving the EEJ variation in the afternoon sector, TEC, and VHF scintillation in the postsunset hours is made to develop a coherent picture of low-latitude ionosphere. The duration of scintillation at VHF is recorded to be nearly half an hour to more than 3 h in multiple patches with an abrupt rise in the S_4 level. Maximum S_4 levels are recorded in the range ~ 0.8–1.2. Onset of ESF near the magnetic equator is detected prior to the initiation of scintillation around RPMC in all cases and is followed by the secondary enhancement in EEJ.

VHF (250 MHz) scintillation is observed for ~ 74% cases on the days with secondary enhancement in EEJ and the same is recorded for ~ 75% cases following secondary enhancement in TEC. It should be mentioned that low-latitude scintillations around the crest region are mainly produced by irregularities in electron density distribution generated near the magnetic equator. Once generated, the irregularities in the form of bubble move upward and map down along the magnetic field lines to off equatorial locations. The low-latitude extension of the irregularity belt is the manifestation of altitudinal extension over the magnetic equator. The irregularities may also have motion in zonal direction. Generation near the magnetic equator does not ensure, in all cases, appearance near the EIA crest owing to finite lifetime and dynamics. Moreover, there is a longitude difference between the EEJ and scintillation observation stations limiting the point-to-point correspondence.

Near the EIA crest injection of electron density irregularities in an environment of high ambient ionization produces strong scintillation. The signature of persistence of high ambient ionization is obtained from diurnal variation of TEC in the postsunset hours. Earlier investigations [*Chakraborty et al.*, 1999] reported a close association between postsunset enhancement in TEC and scintillations near the anomaly crest in the equinoctial months of a high solar activity year. In the present study, amplitude of TEC enhancement appears to be an important parameter to dictate the occurrence of scintillations near the EIA crest. Whenever ΔN_{TEC} exceeds a critical value ~ 6 TECU, scintillation is recorded at RPMC on 80% cases.

Scintillation near the EIA crest is mostly produced by irregularities embedded within the plasma bubble. The signature of bubble is obtained from the temporal variations in TEC on some satellite tracks lying around the VHF I.P.P locations near the EIA crest region. In 67% cases TEC depletions are recorded on days involving secondary enhancement in EEJ. A statistical analysis for any probable correspondence between perturbations in the late afternoon equatorial electric field, as revealed through the EEJ data, and the magnitude of plasma depletion in postsunset hours shows a statistically significant correlation ~ 0.81 between the ΔH_{EEJ} parameter and the depletion magnitude (Figure 6). The secondary enhancement of EEJ, initiated in afternoon period and sustaining up to presunset hours, is found to be an important index to signify the postsunset evolution of equatorial plasma bubble.

The persistence of high ambient ionization contributed by the intense fountain effect and injection of equatorial irregularities are the major components for postsunset scintillation near the EIA crest. Predictability of scintillation around the northern crest of EIA is also attempted on the basis of secondary enhancements in EEJ and in the ambient ionization levels (Figure 7). The occurrence probability is lowest (≈ 47% only) for quadrant (1),

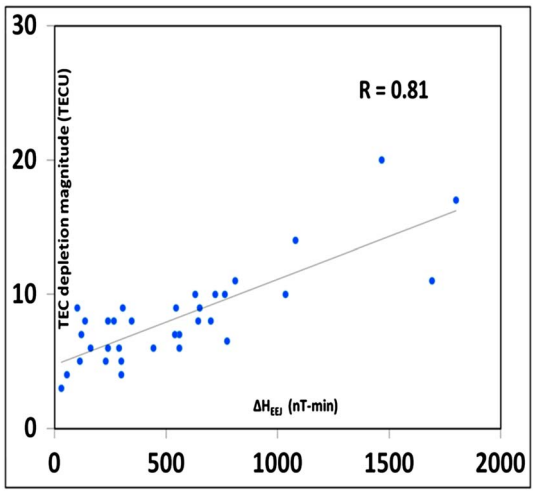

Figure 6. Variation of TEC depletion amplitude obtained along the GNSS satellite track around RPMC versus ΔH_{EEJ} parameter.

when both ΔH_{EEJ} and ΔN_{TEC} are lower than a critical value ~ 400 nT and ~ 6 TECU, respectively. However, scintillation occurrence probability is the highest (~ 86%) when both the afternoon EEJ and postsunset background ionization exhibit secondary enhancement exceeding the stated limits. All the results are statistically significant.

An attempt is made to validate the results of association analysis involving afternoon enhancement of EEJ field and subsequent electrodynamical processes leading to the generation of electron density irregularities responsible for scintillation near the EIA crest. For this VHF (244 MHz) scintillation data during the equinoctial months of high solar activity years (1989–1990), pertaining to solar cycle 22, are analyzed in conjunction with TEC, magnetometer, and ionosonde data. TEC data are obtained using Faraday rotation technique. The scintillation and TEC data are recorded at Calcutta (geographic latitude: 22.58°N, longitude: 88.38°E, dip: 32°) situated near the northern EIA crest. Data are available for 47 and 77 days of the equinoctial months for the years 1989 and 1990, respectively, when normal EEJ and quiet geomagnetic conditions prevailed. During the period solar flux $F_{10.7}$ varies in the range ~ 139–242 solar flux units (10^{-22} W m^{-2} Hz^{-1}). It is observed that there are 35 (66) cases of secondary enhancement in EEJ during afternoon to early evening hours around 1430–1730 IST h in 1989 (1990). Available ionosonde data from equatorial station, Kodaikanal (geographic latitude: 10.2°N, longitude: 77.5°E) reveals ~ 88% (~ 78%) cases of prereversal enhancement (PRE) in the plasma drift near the magnetic equator during postsunset period on days with secondary enhancement in EEJ during 1989 (1990). Also a secondary enhancement in ambient ionization level in postsunset period near the northern crest of EIA is evident in diurnal TEC profile. In most of the cases the secondary enhancement in TEC follows the onset of PRE preceded by the afternoon enhancement in EEJ.

Further occurrence of VHF scintillation near the EIA crest follows the sequence of the secondary enhancement in EEJ, subsequent development of PRE and secondary enhancement in TEC near the EIA crest. Scintillations are recorded for 94% (70%) cases of EEJ intensification, satisfying the conditions $\Delta H_{EEJ} > 400$ nT/min and $\Delta N_{TEC} > 6$ TECU. It may be noted that there are only 4 (5) cases during the observation period of 1989 (1990) when scintillation is recorded near EIA crest in postsunset to premidnight hours without the prior signature of postafternoon secondary enhancement in EEJ. Nonscintillation days are observed to be associated with ΔH_{EEJ} and ΔN_{TEC} parameter < 360 nT/min and < 7 TECU in majority of cases. The result is consistent with those obtained from investigations pertaining to the equinoctial months of 2011–2012.

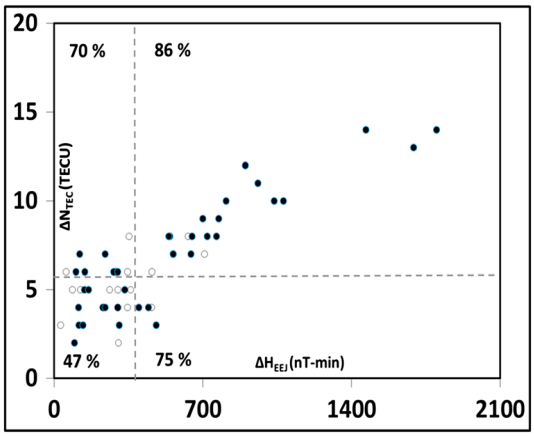

Figure 7. Plot of ΔH_{EEJ} and ΔN_{TEC} parameters for scintillation days (filled circle) and nonscintillation days (empty circle). Threshold values of $\Delta H_{EEJ} > 400$ nT/min and $\Delta N_{TEC} > 6$ TECU are found to be efficient indicator of occurrence of postsunset scintillation near the EIA crest.

During the equinoctial months of 1989 and 1990, the latitudinal variations of ion density are analyzed using Defense Meteorological Satellite Program (DMSP) F8 and F9 satellites with equator crossing time 1800 IST and 2130 IST, respectively, within the longitudinal span of ~ 72°E–90°E. No significant distinguishing features in the ion density data are revealed during scintillation and nonscintillation days around 1800 LT (F8), while the ion density data at 2130 IST (F9) registered distinguishing differences. Figure 8 depicts days of

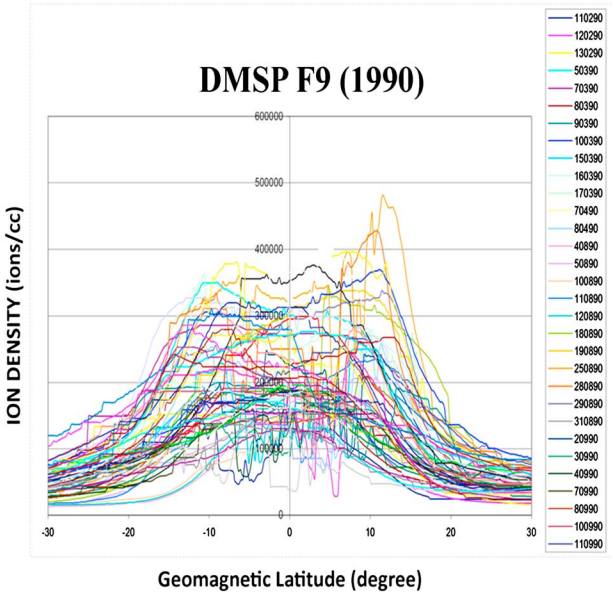

Figure 8. Latitudinal variations of DMSP ion density in 1990 for F9 DMSP satellite. Scintillation days reveal bite-outs/fluctuations around 2130 IST. The right side legend represents the dates of observations when afternoon enhancement in EEJ is occurred. Magnetic equator crossing time is around 2130 IST (h). The latitudinal variations of the ion density corresponding to 88° ± 5°E longitude zone have only been considered.

the year 1990 which are associated with afternoon secondary enhancement in EEJ preceding the onset of PRE and subsequent occurrence of VHF scintillation. It may be noticed from the figure that on these days, the ion density exhibits bite-outs or fluctuating depletions (F9). Also, it is observed for majority of cases that the higher latitudinal width, greater peak values, and symmetrical distributions of EIA differentiate the scintillation days from the nonscintillation ones.

4. Discussions

The observational results may be discussed on the basis of sequential electrodynamical effects developed following afternoon enhancements in EEJ. The equatorial *E* region ionosphere plays a decisive role in determining the electric fields in the ionosphere for several hundreds of kilometers above it during the evening hours [*Haerendel and Eccles*, 1992]. On a day when *E* layer dynamo electric field is well developed, the *F* layer dynamo responsible for prereversal enhancement (PRE) of eastward electric field, an important factor for postsunset triggering of ESF [*Rishbeth*, 1971; *Farley et al*., 1986; *Heelis*, 2004], is reported to also be developed prominently [*Abdu*, 2001]. For the development of PRE, *E* region condition is more important than the *F* region conditions [*Kil and Oh*, 2011]. *Kelley et al*. [2009] suggested that PRE must be created by EEJ current closure. EEJ strength is considered as a proxy index of equatorial *E* region electric field [*Anderson et al*., 2002; *Stolle et al*., 2008] driven by *E* layer dynamo. Following a case study during vernal equinoctial months of 2011, *Hajra et al*. [2012] asserted that the variation of EEJ after 1530 IST (h) may play a crucial role in dictating the postsunset resurgence of EIA and triggering of ESF. In the present investigation a comparatively larger database is used for identifying suitable parameters which may be treated as precursor for postsunset occurrence of density irregularities and subsequent occurrence of equatorial scintillation near the EIA crest. It is revealed that ΔH_{EEJ} parameter which synthesizes both the magnitudes and duration of elevated afternoon EEJ, not the secondary peak magnitude, may be treated as an important index for postsunset resurgence of EIA and evolution of equatorial density irregularities. Both the ΔH_{EEJ} parameter and ΔN_{TEC}, implying secondary enhancement magnitudes of TEC near the EIA crest, are found to be important indices with corresponding threshold values for occurrence of equatorial scintillation. The results are validated using database of earlier high solar activity years.

The secondary enhancement of EEJ may directly be attributed to the variability of *E* region eastward electric field as the contribution of conductivity variation may assume to be negligible [*Stolle et al*., 2008]. The afternoon enhancement in EEJ field and its sustenance may accentuate the fountain effect thereby intensifying the EIA processes around the sunset period. A series of sequential dynamical processes conducive for development of *F* region irregularities may initiate following intensification of EIA structure. In a climatological sense PRE is the most important parameter controlling the generation of ESF at solar maxima [*Abdu et al*., 1983; *Fejer et al*., 1999; *Chapagain et al*., 2009]. PRE is developed due to *F* region dynamo which may again be discussed either by invoking (i) modification of thermospheric zonal wind component or (ii) current continuity requirement. A feedback mechanism between enhanced EIA and PRE is suggested by *Prakash et al*. [2009]. The enhanced EIA can reduce (increase) the drag on neutrals enhancing the zonal wind and its local time gradient at the equatorial latitudes (the anomaly crest latitudes)—an important component for postsunset development of *F* region dynamo [*Crain et al*., 1993b; *Sastri*, 1998; *Chapagain et al*., 2013]. It may facilitate formation of equatorial temperature and wind anomaly vis-à-vis

meridional circulation cell of thermospheric wind [*Raghavarao et al.*, 1991]. A possibility exists that EIA and ESF are linked through the meridional circulation cells and the associated vertical winds. The vertical winds (downward/upward) are capable of altering (enhancing/inhibiting) the growth of the primary R-T instability [*Sekar et al.*, 1994]. The effect of vertical wind in the development of ESF is important only in the presence of finite field line integrated Pedersen conductivity [*Hysell et al.*, 1990]. The strengthening of the plasma fountain driven by enhanced EEJ field will enhance the ratio of flux tube integrated Pedersen conductivity of the *F* to *E* region, in view of the increased plasma content along the flux tubes with high-apex altitudes over the magnetic equator [*Crain et al.*, 1993a]. The said changes into the upper atmosphere may thus constitute favorable conditions for effective *F* region dynamo action. Further, the coupling between *E* and *F* layers around the solar terminator is explained as a spillover of the dayside equatorial electrojet into the *F* layer [*Haerendel and Eccles*, 1992; *Denardini et al.*, 2006]. Afternoon evolution and sustenance up to presunset hours of enhanced EEJ may facilitate the efficient coupling by developing ambient conditions suitable for meeting the necessary *F* region current demand.

All the hierarchical changes in the equatorial upper atmosphere seem to instigate by the afternoon enhancement of EEJ to set up favorable conditions for a very efficient *F* region dynamo action, a necessary condition for triggering the *F* region irregularity through the development of PRE over the magnetic equator, provided that other conditions are omnipresent.

Ionospheric irregularities in the postsunset equatorial ionosphere are embedded within the plasma density depletions, commonly known as bubbles. These are produced over the magnetic equator at the bottom side of *F* layer through plasma instability mechanisms and rise to the topside ionosphere [*Woodman and La Hoz*, 1976]. Plasma drift and the height of the *F* layer are reported to be the important factors facilitating generation of plasma bubbles [*Huang et al.*, 2012]. A larger vertical plasma drift driven by PRE at the magnetic equator in the postsunset period is responsible for the larger-scale TEC depletions in the EIA region [*Abdu et al.*, 2008]. A good correlation between the depth of TEC depletions and ΔH_{EEJ} parameters may result from the intensification of PRE instigated by enhanced EEJ. As the bubbles move upward it also down drafted along the magnetic field lines to the off equatorial locations. After onset over the magnetic equator the bubbles reach the highest altitudes/latitudes only on these days when a postsunset secondary enhancement in TEC is observed there [*Dabas et al.*, 2003] and the polarity of EEJ is not reversed [*Hysell and Burcham*, 1998]. A strong PRE leads to the resurgence of EIA thereby facilitating development of secondary enhancement in TEC halting the normal postsunset decay process.

Thus, afternoon enhancement and sustenance of electric field, as revealed through the diurnal variation of EEJ, appears to be an important precursor for initializing all the electrodynamical processes leading to evolution of equatorial irregularities and subsequent occurrence of scintillations near the EIA crest.

5. Conclusion

Investigation of equatorial electrojet (EEJ) data in conjunction with scintillation and TEC data near the EIA crest and ionosonde data from an equatorial station reveal that afternoon enhancement following the diurnal maximum of EEJ may be considered as an important index for postsunset evolution of equatorial irregularities and subsequent occurrence of scintillation. Following secondary enhancement of EEJ, a number of sequential electrodynamical effects such as resurgence of EIA structure and secondary enhancement in TEC near the EIA crest are observed. Both the magnitude and duration of enhanced EEJ, which actually signify sustenance of elevated electric field strength over the magnetic equator, are found to be important parameter to accentuate all the above mentioned electrodynamical processes. Occurrence of intense scintillation near the EIA crest is conditioned by the persistence of high ambient ionization level. Information regarding the high ambient level near EIA crest is manifested through the secondary enhancement of TEC (ΔN_{TEC}). The critical values of ΔH_{EEJ} parameter, which includes the magnitude and duration of enhanced EEJ and of ΔN_{TEC}, secondary enhancement magnitude of TEC, may fruitfully be utilized as precursor for triggering post-sunset equatorial scintillation near the EIA crest during high solar activity years.

It should be mentioned that the results accrued pertain to observations on equinoctial months of high solar activity years only. To employ an effective forecasting parameter seasonal- and solar activity-dependent features of the same are to be investigated as well.

Acknowledgments

The work has been carried out with the financial assistance of the Department of Science and Technology, Government of India, under SERB project. The authors are thankful to A. Dasgupta, C.U., for providing scintillation (244 MHz) and TEC data of Calcutta for the period 1989–1990 and for his valuable suggestions. For C/NOFS ion density data the authors are thankful to P. Roddy, Air Force Research Laboratory, Kirtland Air Force Base, New Mexico, USA. Ionosonde data for the earlier years (1989–1990) were collected from J.H. Sastri, IIA, Bangalore. IGS TEC data are downloaded from http://cdaweb.gsfc.nasa.gov. DMSP ion density data for the period 1989–1990 were supplied by Marc Hariston, UTDALLAS.

Robert Lysak thanks Nanan Balan and two anonymous reviewers for their assistance in evaluating this paper.

References

Abdu, M. A. (2001), Outstanding problems in the equatorial ionosphere-thermosphere electrodynamics relevant to spread F, *J. Atmos. Sol. Terr. Phys.*, *63*, 869–884.

Abdu, M. A., R. T. de Medeiros, J. A. Bittencourt, and I. S. Batiste (1983), Vertical ionization drift velocities and range type spread F in the evening equatorial ionosphere, *J. Geophys. Res.*, *88*(A1), 339–342.

Abdu, M. A., J. W. MacDougall, I. S. Batista, J. H. A. Sobral, and P. T. Jayachandran (2003), Equatorial evening prereversal electric field enhancement and sporadic E layer disruption: A manifestation of E and F region coupling, *J. Geophys. Res.*, *118*(A6), 1254, doi:10.1029/2002JA009285.

Abdu, M. A., E. A. Kherani, I. S. Batista, E. R. de Paula, D. C. Fritts, and J. H. A. Sobral (2008), Abnormal evening vertical plasma drift and effects on EIA and ESF over Brazil-South Atlantic sector during 30 October 2003 super storm, *J. Geophys. Res.*, *113*, A07313, doi:10.1029/2007JA012844.

Akasofu, S. I. (1981), Relationship between the AE and DST indices during geomagnetic storms, *J. Geophys. Res.*, *86*(A6), 4820–4822.

Anderson, D., A. Anghel, K. Yumoto, M. Ishitsuka, and E. Kudeki (2002), Estimating daytime vertical $E \times B$ drift velocities in the equatorial F-region using ground-based magnetometer observations, *Geophys. Res. Lett.*, *29*, 1596, doi:10.1029/2001GL014562.

Balan, N., Y. Otsuka, M. Nishioka, J. Y. Liu, and G. J. Bailey (2013), Physical mechanisms of the ionospheric storms at equatorial and higher latitudes during the recovery phase of geomagnetic storms, *J. Geophys. Res. Space Physics*, *118*, 2660–2669, doi:10.1002/jgra.50275.

Basu, S., S. Basu, J. Aarons, J. P. Mcclure, and M. D. Cousins (1978), On the coexistence of kilometre- and meter-scale irregularities in the night time equatorial F region, *J. Geophys. Res.*, *83*(A9), 4219–4226.

Basu, S., E. M. MacKenzie, S. Basu, E. Costa, P. F. Fougere, H. C. Carlson Jr., and H. E. Whiteney (1987), 250MHz/GHz scintillation parameters in the equatorial, polar and auroral environments, *IEEE J. Selec. Areas Commun.*, *SAC-5*, 102.

Basu, S., et al. (1996), Scintillations, plasma drifts, and neutral winds in the equatorial ionosphere, *J. Geophys. Res.*, *101*, 26,783–26,795.

Basu, S., K. M. Groves, S. Basu, and P. J. Sultan (2002), Specification and forecasting of scintillations in communication/navigation links: Current status and future plans, *J. Atmos. Sol. Terr. Phys.*, *64*, 1745–1754.

Basu, S., S. Basu, J. Huba, J. Krall, S. E. McDonald, J. J. Makela, E. S. Miller, S. Ray, and K. Groves (2009), Day-to-day variability of the equatorial ionization anomaly and scintillations at dusk observed by GUVI and modeling by SAMI3, *J. Geophys. Res.*, *114*, A04302, doi:10.1029/2008JA013899.

Bittencourt, J. A., and M. A. Abdu (1981), A theoretical comparison between apparent and real vertical ionization drift velocities in the equatorial F region, *J. Geophys. Res.*, *86*(A4), 2451–2454.

Chakraborty, S. K., and R. Hajra (2009), Electrojet control of ambient ionization near the crest of the equatorial anomaly in the Indian zone, *Ann. Geophys.*, *27*, 93–105.

Chakraborty, S. K., A. Dasgupta, S. Ray, and S. Banerjee (1999), Long-term observations of VHF scintillations and total electron content near the crest of the equatorial anomaly in the Indian longitude zone, *Radio Sci.*, *34*(1), 241–255.

Chandra, H., and R. G. Rastogi (1974), Geomagnetic storm effects on ionospheric drifts and the equatorial Es over the magnetic equator, *Ind. J. Radio Space Phys.*, *3*, 332–336.

Chapagain, N. P., B. G. Fejer, and J. L. Chau (2009), Climatology of post sunset equatorial spread F over Jicamarca, *J. Geophys. Res.*, *114*, A07307, doi:10.1029/2008JA013911.

Chapagain, N. P., D. J. Fisher, J. W. Meriwether, J. L. Chau, and J. J. Makela (2013), Comparison of zonal neutral winds with equatorial plasma bubble and plasma drift velocities, *J. Geophys. Res. Space Physics*, *118*, 1802–1812, doi:10.1002/jgra.50238.

Cowling, T. G. (1933), The electrical conductivity of an ionized gas in the presence of a magnetic field, *Mon. Not. R. Astron. Soc.*, *93*, 90–98.

Crain, D. J., R. A. Heelis, and G. J. Bailey (1993a), Effects of electrical coupling on equatorial ionosphere plasma motions: When the F region a dominant driver in low latitude dynamics, *J. Geophys. Res.*, *98*, 6033–6037.

Crain, D. J., R. A. Heelis, G. J. Bailey, and A. D. Richmond (1993b), Low-latitude plasma drifts from a simulation of the global atmospheric dynamo, *J. Geophys. Res.*, *98*(A4), 6039–6046.

Dabas, R. S., and B. M. Reddy (1986), Nighttime VHF scintillations at 23°N magnetic latitudes and their association with equatorial F region irregularities, *Radio Sci.*, *21*, 453–462.

Dabas, R. S., L. Singh, D. R. Lakshmi, P. Subramanyam, P. Chopra, and S. C. Garg (2003), Evolution and dynamics of equatorial plasma bubbles: Relationships to $E \times B$ drift, postsunset total electron content enhancements, and equatorial electrojet strength, *Radio Sci.*, *38*, 1075, doi:10.1029/2001RS002586.

de La Beaujardière, O., and the C/NOFS Definition Team (2004), C/NOFS: A mission to forecast scintillations, *J. Atmos. Sol.-Terr. Phys.*, *66*, 1573, doi:10.1016/j.jastp.2004.07.030.

Denardini, C. M., M. A. Abdu, E. R. de Paula, C. M. Wrasse, and J. H. A. Sobral (2006), VHF radar observations of the dip equatorial E-region during sunset in the Brazilian sector, *Ann. Geophys.*, *24*, 1–7.

Deshpande, M. R., et al. (1977), Effect of electrojet on total electron content of the ionosphere over the Indian sub-continent, *Nature*, *267*, 599–600.

Farley, D. T., B. B. Balsley, R. F. Woodman, and J. P. McClure (1970), Equatorial spread F: Implications of VHF radar observations, *J. Geophys. Res.*, *75*, 7199–7216.

Fejer, B. G., L. Scherliess, and E. R. de Paula (1999), Effects of the vertical plasma drift velocity on the generation and evolution of equatorial spread F, *J. Geophys. Res.*, *104*, 19,859–19,869.

Fesen, C. G., G. Crowley, R. G. Roble, and A. D. Richmond (2000), Simulation of the pre-reversal enhancement in the low latitude vertical ion drifts, *Geophys. Res. Lett.*, *27*(13), 1851–1854.

Haerendel, G., and J. V. Eccles (1992), The role of the equatorial electrojet in the evening ionosphere, *J. Geophys. Res.*, *97*, 1181–1192.

Hajra, R., S. K. Chakraborty, and A. Paul (2009), Electrodynamical control of the ambient ionization near the equatorial anomaly crest in the Indian zone during counter-electrojet days, *Radio Sci.*, *44*, RS3009, doi:10.1029/2008RS003904.

Hajra, R., S. K. Chakraorty, S. Mazumdar, and S. Alex (2012), Evolution of equatorial irregularities under varying electrodynamical conditions: A multi-technique case study from Indian longitude zone, *J. Geophys. Res.*, *117*, A08331, doi:10.1029/2012JA017808.

Heelis, R. A. (2004), Electrodynamics in the low and middle latitude ionosphere: A tutorial, *J. Atmos. Sol. Terr. Phys.*, *66*, 825–838.

Huang, C.-S., O. de La Beaujardiere, P. A. Roddy, D. E. Hunton, J. O. Ballenthin, and M. R. Hairston (2012), Generation and characteristics of equatorial plasma bubbles detected by the C/NOFS satellite near the sunset terminator, *J. Geophys. Res.*, *117*, A11313, doi:10.1029/2012JA018163.

Hysell, D. L., and J. Burcham (1998), JULIA radar studies of equatorial spread F, *J. Geophys. Res.*, *103*, 29,155–29,167, doi:10.1029/98JA02655.

Hysell, D. L., M. C. Kelley, W. E. Swartz, and R. F. Woodman (1990), Seeding and layering of equatorial spread F by gravity waves, *J. Geophys. Res.*, *95*, 17,253–17,260.

Kelley, M. C. (1989), *The Earth's Ionosphere Plasma Physics and Electrodynamics*, International Geophysics Series, vol. 43, Academic Press, San Diego, Calif.

Kelley, M. C., R. R. Ilma, and G. Crowley (2009), On the origin of pre-reversal enhancement of the zonal equatorial electric field, *Ann. Geophys.*, *27*, 2053–2056.
Kil, H., and S. J. Oh (2011), Dependence of the evening prereversal enhancement of the vertical plasma drift on geophysical parameters, *J. Geophys. Res.*, *116*, A05311, doi:10.1029/2010JA016352.
MacDougall, J. W. (1969), The equatorial ionospheric anomaly and the equatorial electrojet, *Radio Sci.*, *4*, 805–810.
McDonald, S. E., C. Coker, K. F. Dymond, D. N. Anderson, and E. A. Araujo-Pradere (2011), A study of the strong linear relationship between the equatorial ionization anomaly and the prereversal E × B drift velocity at solar minimum, *Radio Sci.*, *46*, RS6004, doi:10.1029/2011RS004702.
Park, J., H. Luhr, and K. W. Min (2010), Characteristic of F-region dynamo currents deduced from CHAMP magnetic field measurements, *J. Geophys. Res.*, *115*, A10302, doi:10.1029/2010JA015604.
Prakash, S., D. Pallamraju, and H. S. S. Sinha (2009), Role of the equatorial ionization anomaly in the development of the evening prereversal enhancement of the equatorial zonal electric field, *J. Geophys. Res.*, *114*, A02301, doi:10.1029/2007JA012808.
Raghavarao, R., M. Nageswararao, J. H. Sastri, G. D. Vyas, and M. Sriramarao (1988), Role of equatorial ionization anomaly in the initiation of equatorial spread F, *J. Geophys. Res.*, *93*, 5959–5964, doi:10.1029/JA093iA06p05959.
Raghavarao, R., L. E. Wharton, N. W. Spencer, H. G. Mayr, and L. H. Brace (1991), An equatorial temperature and wind anomaly (ETWA), *Geophys. Res. Lett.*, *18*, 1193–1196.
Rastogi, R. G., and J. A. Klobuchar (1990), Ionospheric electron content within the equatorial F2 layer anomaly belt, *J. Geophys. Res.*, *95*, 19,045–19,052.
Ray, S., A. Paul, and A. Dasgupta (2006), Equatorial scintillations in relation to ionization anomaly, *Ann. Geophys.*, *24*, 1429–1442.
Rishbeth, H. (1971), Polarization fields produced by winds in the equatorial F-region, *Planet. Space Sci.*, *19*, 357–369.
Sastri, J. H. (1998), On the development of abnormally large postsunset upward drift of equatorial F region under quiet geomagnetic conditions, *J. Geophys. Res.*, *103*, 3983–3991.
Sekar, R., R. Suhasini, and R. Raghavarao (1994), Effects of vertical winds and electric fields in the nonlinear evolution of equatorial spread F, *J. Geophys. Res.*, *99*, 2205–2213.
Sethia, G., R. G. Rastogi, M. R. Deshpande, and H. Chandra (1980), Equatorial electrojet control of the low latitude ionosphere, *J. Geomag. Geoelectr.*, *32*, 207–216.
Somayajulu, Y. V., S. C. Garg, R. S. Dabas, L. Singh, T. R. Tyagi, B. Lokanadham, S. Ramakrishna, and G. Navneeth (1984), Multistation study of nighttime scintillations in low latitudes: Evidence of control by equatorial F region irregularities, *Radio Sci.*, *19*(3), 707–718.
Sridharan, R., D. Pallam Raju, R. Raghavarao, and P. V. S. Ramarao (1994), Precursor to equatorial spread-F in OI 630.0 nm dayglow, *Geophys. Res. Lett.*, *21*, 2797–2800.
Stolle, C., C. Manoj, H. Luhr, S. Maus, and P. Alken (2008), Estimating the daytime equatorial ionization anomaly strength from electric field proxies, *J. Geophys. Res.*, *113*, A09310, doi:10.1029/2007JA012781.
Uemoto, J., T. Maruyama, S. Saito, M. Ishii, and R. Yoshimura (2010), Relationships between PRE-sunset electrojet strength, pre-reversal enhancement and equatorial spread-F onset, *Ann. Geophys.*, *28*, 449–454.
Whalen, J. A. (2000), An equatorial bubble: Its evolution observed in relation to bottomside spread F and to the Appleton anomaly, *J. Geophys. Res.*, *105*, 5303–5315.
Whalen, J. A. (2003), Dependence of the equatorial anomaly and of equatorial spread F on the maximum prereversal E X B drift velocity measured at solar maximum, *J. Geophys. Res.*, *108*(A5), 1193, doi:10.1029/2002JA009755.
Whitney, H. E., J. Aarons, and C. Malik (1969), A proposed index for measuring ionospheric scintillation, *Planet. Space. Sci.*, *17*, 1069–1073.
Woodman, R. F. (1970), Vertical drift velocities and east–west electric fields at the magnetic equator, *J. Geophys. Res.*, *75*, 6249–6259, doi:10.1029/JA075i031p06260.
Woodman, R. F., and C. La Hoz (1976), Radar observations of F region equatorial irregularities, *J. Geophys. Res.*, *81*, 5447–5466.